*Vedic Science, International Multidisciplinary Peer Reviewed Research Journal*
*Vol. 28, Issue April- June 2026, PP. 125-148*
*ISSN No. 0975-0312*
*DOI: https://doi.org/10.66718/vsj.v28.i2.09*

# The Shape of the Cosmos

## A Tripartite Electrodynamic Architecture of the Info Magneto Electrostatic (IME) Cosmos

**Dr Satinder Singh Malik**

Independent Researcher in Foundations of Physics and Philosophy of Science

ORCID: 0000-0002-6743-2102

## Abstract

This treatise presents a unified, multi-disciplinary re-evaluation of the global architecture of the cosmos, synthesising the ontological framework of the Upanishadic triad of Gunas (Sattva, Rajas, and Tamas) with a hydrodynamic and electrodynamic model of celestial mechanics. The central thesis is that the cosmos is a finite, three-layered, nested structure. The outermost layer is an energetically spherical boundary woven from an information matrix of space-filling rhombic dodecahedral cells (the *Sattvic* grid). Enclosed within it is a toroidal magnetic drive system (the Rajasic torus) whose major-to-minor radius proportion embodies the golden ratio phi while its circulatory geometry embodies pi, jointly expressing the harmonic design constants observed throughout cosmic structure. Innermost lies a flat, hollow equatorial disc (the Tamasic Cosmic Chakra) upon which all visible baryonic matter floats, held in its plane by the pinch effect of the confining magnetic flux. Space is modelled as a compressible celestial plenum of variable permittivity; gravity is reinterpreted as an adhesive plenum pressure gradient governed by a kinematic Plenum Influence Parameter, and mass is treated as bipartite (an inert Mahatva and an interactive Gurutva). The model derives the Chakra Confinement Equation that balances plenum expansion pressure against magnetic confinement pressure, a convergent volumetric series that yields a finite cosmos from an infinitely resolved interior, and a variable speed of light that explains cosmological redshift as refractive deceleration rather than metric expansion. The absolute cosmic boundary is derived from first principles using the Nested Pressure Model, which empirically calibrates the inverse-square decay of plenum pressure across the planetary, stellar, and galactic vortex tiers and then releases the uncontained central cosmic vortex from artificial compression. This yields a Vortex Horizon of approximately 22.8 billion light-years for the full mass-energy anchor, partitioned by an area-proportional law into a stratified radial disc: a dense visible cosmos extending to about 5.1 Gly, a bipartite or dark-matter halo from 5.1 to 12.1 Gly, and a pure fluid plenum extending to the outer mirror boundary at 22.8 Gly. The framework is consistent with the Planck 2018 preference for a closed universe, the Hubble tension, large-scale bulk flows, and the recently confirmed rotation of cosmic filaments. It yields explicit, falsifiable predictions and is offered as a rigorous philosophical scaffold for

future observational programmes.

## Keywords

Toroidal cosmos, celestial plenum, Tripartite ontology, rhombic dodecahedral grid, magnetic Z-pinch, Cosmic Chakra, Plenum Influence Parameter, Nested Pressure Model, Vortex Horizon, stratified radial disc, bipartite mass, variable permittivity, golden-ratio torus, holographic boundary, cosmological redshift, closed universe

## 1. Introduction

### 1.1 The Problem of Cosmic Shape

The question of the shape and extent of the cosmos is among the oldest in natural philosophy and remains unresolved in contemporary cosmology. The standard Lambda Cold Dark Matter (LambdaCDM) model assumes a spatially flat, isotropic, and homogeneous universe as a mathematically convenient background, yet this assumption is now under pressure from several independent observational fronts. The Planck 2018 legacy data release reported an anomalous gravitational lensing amplitude that favours a positively curved, closed universe at greater than 99 percent confidence (Di Valentino et al., 2020). Independent Bayesian analysis found betting odds of approximately 50 to 1 against a flat universe from the cosmic microwave background data alone (Handley, 2021). The persistent Hubble tension, large-scale bulk flows extending without convergence beyond 200 megaparsecs, and the recently confirmed coherent rotation of cosmic filaments spanning tens of millions of light-years all suggest that the cosmos possesses a structured global architecture that the standard model does not capture (Libeskind et al., 2021).

This paper addresses these anomalies by proposing a specific, finite, three-layered architecture for the cosmos and by replacing the philosophical foundations of the standard model rather than patching its parameters. It is a substantial revision and extension of two earlier manuscripts by the present author on celestial mechanics and dimensional ontology (Malik, 2025, 2026), incorporating a newly developed Tripartite anatomy of the central cosmic engine.

### 1.2 The Semantic Distinction between Universe and Cosmos

A persistent source of confusion is the conflation of the terms universe and cosmos. Etymologically, the prefix uni- (one) in universe denotes a singular unit, a single verse, appropriately applied to one galaxy. The word cosmos, from the Greek kosmos meaning order or ordered arrangement, denotes the harmonious totality of all such units. The distinction is not merely verbal: it implies that the cosmos has a structured, ordered architecture that single-galaxy models cannot describe. Throughout this paper, cosmos refers to the bounded, ordered totality, and universe refers to a constituent galactic unit within it.

### 1.3 Methodology: Upmana and Analogical Inference

The methodological backbone of this work is Upmana, the third valid source of

knowledge (pramana) in classical Indian epistemology, which constructs knowledge of inaccessible vast systems by rigorous structural comparison with accessible smaller analogues. The logical warrant for this procedure is the empirically supported scale invariance of the governing fluid-dynamical equations: the same mathematical forms describe an electron bound to a proton, a planet bound to a star, and a star bound to a galactic centre. Upmana is therefore not loose analogy but a disciplined appeal to structural isomorphism across scales.

## 2. The Tripartite Ontological Framework

The architecture proposed here rests on an ontological mapping between the three Gunas of Samkhya philosophy and three physically distinct operational regimes of the cosmos. The Gunas are the three fundamental constituent qualities of manifest reality described in Samkhya Karika and the Bhagavad Gita: Sattva (clarity, intelligence, geometric order), Rajas (activity, motion, dynamism), and Tamas (inertia, density, substance). The present framework interprets these not as moral or psychological categories but as the three operative physical attributes of cosmic energy.

| Guna | Ontological Role | Physical Realisation | Cosmic Layer |
|---|---|---|---|
| Sattva | Information, geometry, intention | Frictionless rhombic-dodecahedral spatial grid; the conserved geometric blueprint | Layer 1: Outer information sphere |
| Rajas | Motion, activity, cyclic drive | Sweeping magnetic flux forming a toroidal dynamo; the active torque carrier | Layer 2: Magnetic torus |
| Tamas | Inertia, density, substance | Compressible dielectric quantum foam condensing into baryonic matter | Layer 3: Equatorial baryonic disc |

Table 1. The Tripartite mapping between the three Gunas of Samkhya ontology and the three physical layers of the cosmos.

### 2.1 The Five Fundamental Domains

The Tripartite mapping is embedded within a broader five-domain ontology developed in earlier work (Malik, 2025). Any physical entity is fully specified by a quintuple of irreducible domains: Space, Time, Energy, Matter, and Information. In the present framework, Sattva corresponds to the Information domain, Rajas to the Energy domain in its active magnetic mode, and Tamas to the Matter domain. Space and Time provide the arena. A physical object O is therefore written as the tuple of equation (1):

$$O = ( s \in S,\ t \in T,\ e \in E,\ m \in M,\ i \in I ) \qquad (1)$$

where S, T, E, M, and I denote the Space, Time, Energy, Matter, and Information domains respectively. The framework asserts that no four-domain specification is ontologically complete; the Information domain (Sattva) is required to close the

description of any ordered system, in agreement with the information-theoretic foundations of physics articulated by Wheeler (1990) and the integrated-information formalism of Tononi (2008).

## 3. The Three-Layer Cosmic Architecture

The central structural claim of this paper is that the cosmos is a finite, nested, three-layer system. From the outside inward, these layers are the *Sattvic* information sphere, the Rajasic magnetic torus, and the Tamasic baryonic disc. Each layer is the physical realisation of one Guna, and each performs a distinct mechanical function in the cosmic engine. Figure 1 presents the schematic of this architecture.

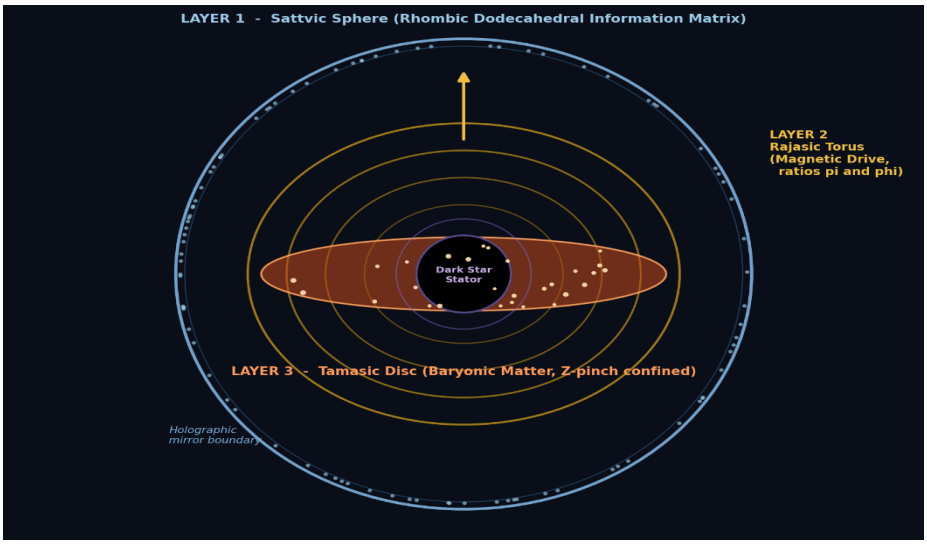


Figure 1. Schematic of the three-layer cosmic architecture. Layer 1 (outer) is the spherical Sattvic information matrix; Layer 2 (middle) is the Rajasic magnetic torus that provides the drive and confinement; Layer 3 (inner) is the flat Tamasic baryonic disc. The central Dark Star stator anchors the entire system.

### 3.1 Layer 1: The *Sattvic* Information Sphere

The outermost layer is, in theoretical idealisation, a perfect sphere. It is not a sphere of material substance but a sphere of energy and information: a space-filling matrix of rhombic dodecahedral cells that constitutes the geometric blueprint of the cosmos. The justification for sphericity at this layer is the inverse-square propagation law. Energy emitted from a central source spreads as an expanding spherical wavefront, so a closed energy boundary is necessarily spherical. This layer is *Sattvic*: it is frictionless, unmoving, and purely informational. It establishes the boundary conditions and the conservation laws within which all cosmic activity unfolds. Its detailed geometry is developed in Section 4.

### 3.2 Layer 2: The Rajasic Magnetic Torus

Enclosed within the information sphere is the active drive layer: a toroidal structure of magnetic flux lines. This is the Rajasic layer, the cosmic dynamo. Magnetic field lines erupt from the polar cusps of the central stator, loop through deep space, and plunge back into the opposite pole, tracing a torus. This toroidal magnetic field is the

active driver of the cosmos: it torques downstream celestial bodies, transmits angular momentum, and, critically, confines the baryonic matter into a flat disc by the pinch effect described in Section 6. The geometry of this torus embodies the two great

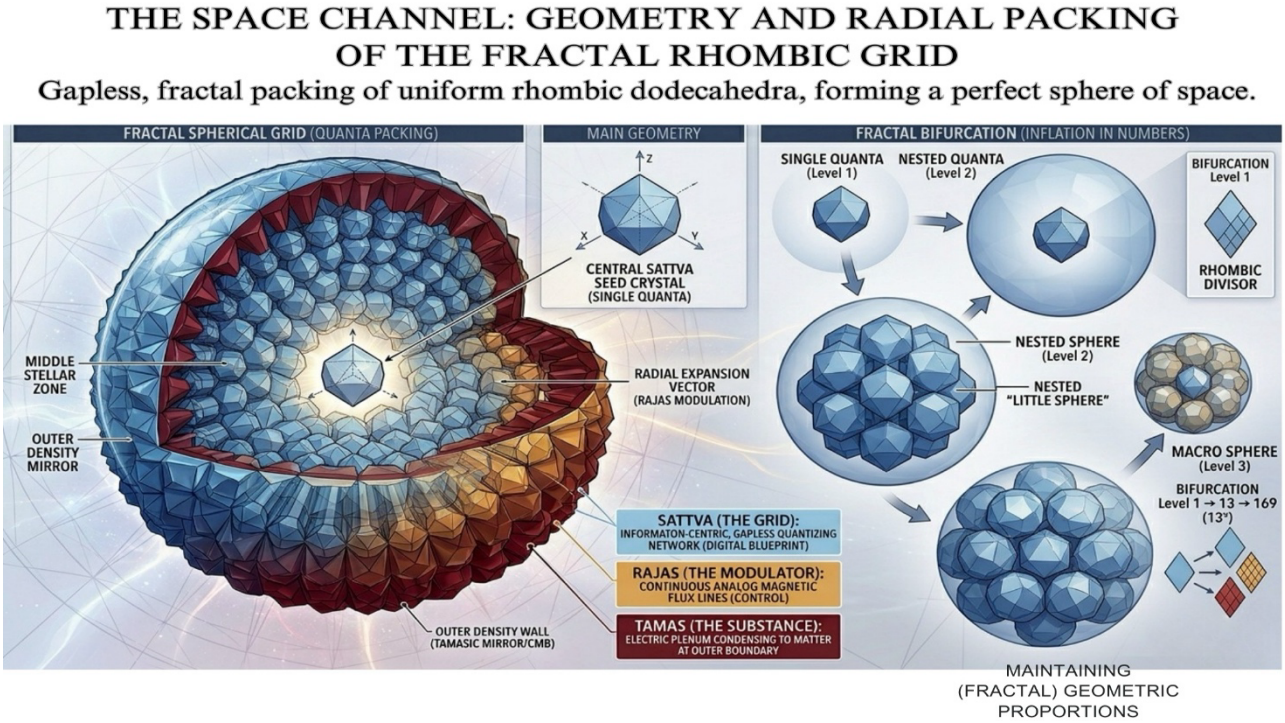


harmonic constants of nature, pi and the golden ratio phi, as developed in Section 5.

### 3.3 Layer 3: The Tamasic Baryonic Disc

Innermost is a flat, hollow equatorial disc. This is the Tamasic layer: the Cosmic Chakra. All visible baryonic matter, every galaxy and every star, floats upon this disc. The disc is hollow in the sense that its central region is swept clean by the intense magnetic flux of the inner cavity. Matter is held in the equatorial plane not by gravitational attraction in the Newtonian sense but by the pinch effect of the surrounding magnetic flux, which crushes the outward-flowing plenum into a razor-thin sheet. The mechanics of this confinement are derived in Section 6.

Hypothesis H1 (Three-Layer Architecture). The cosmos is a finite, nested, three-layer system: an outer spherical Sattvic information matrix of rhombic dodecahedral cells, a middle Rajasic magnetic torus carrying the harmonic ratios pi and phi, and an inner flat Tamasic baryonic disc confined to its plane by magnetic pinch pressure.

## 4. The *Sattvic* Information Matrix: Rhombic Dodecahedral Geometry

The outer spherical layer is constructed from a space-filling matrix of identical geometric cells. The requirement is a polyhedron that tiles three-dimensional space with zero gaps, scales radially while preserving its proportions, and partitions the full solid angle of 4 pi steradians without residue. The unique solution is the rhombic dodecahedron, a twelve-faced solid whose faces are identical rhombi and which is one of the few convex polyhedra that tiles space with one hundred percent volumetric efficiency. Figure 2 illustrates the fractal radial packing of this grid.

Figure 2. The Sattvic space channel. Geometry and radial packing of the fractal rhombic dodecahedral grid. A central seed crystal is surrounded by twelve identical cells, and the structure scales outward by fractal bifurcation. Conceptual rendering supplied with the source manuscript (Malik, 2026).

### 4.1 Geometry of the Unit Cell

Let a single *Sattvic* unit cell be a rhombic dodecahedron of edge length a. Each of its twelve rhombic faces has an acute angle theta given by equation (2):

$$\theta = \arccos(1/3) \approx 70.53^\circ, \quad \text{obtuse angle} = 109.47^\circ \qquad (2)$$

The diagonals of each rhombic face stand in the ratio square root of two to one, which is precisely the proportion that allows the cells to interlock without shear or residual wedge. The volume of a single unit cell is given by equation (3):

$$V_{quanta} = (16\sqrt{3} / 9)\, a^3 \approx 3.0792\, a^3 \qquad (3)$$

### 4.2 The Base-13 Fractal Clustering Law

When a single seed crystal is placed at the cosmic centre, its twelve faces define twelve primary solid angles radiating outward. To pack the next concentric layer while preserving a spherical clustering profile, exactly twelve identical cells snap onto the twelve faces of the seed, producing a closed thirteen-cell cluster of one central plus twelve surrounding cells. This is the geometric origin of the Base-13 fractal scaling law, equation (4):

$$N(n) = 13^n \qquad \text{(total cells at fractal level n)} \qquad (4)$$

| Fractal Level n | Cells N(n) = 13^n | Structural Interpretation |
|---|---|---|
| 0 (seed) | 1 | Single quantum cell at the cosmic centre |
| 1 | 13 | First closed macro-sphere; local cluster |
| 2 | 169 | Galactic-grid cluster |
| 3 | 2,197 | The Cosmic Rotor sphere of master crystals |

Table 2. The Base-13 fractal clustering law. Each successive structural tier contains thirteen times as many cells as the preceding tier.

### 4.3 The Convergent Volumetric Series

The cosmos must reconcile two apparently opposed requirements: an interior of effectively infinite spatial resolution near the centre and a strictly finite, bounded total volume. The rhombic dodecahedral grid achieves this through a convergent geometric series. As the structure is traversed from the outer boundary inward, the number of cells in each successive layer grows while the volume of each individual cell shrinks. Let the layer index be n, the cell count at layer n be N(n), and the individual cell volume be V(n). The total cosmic volume is the sum in equation (5):

$$V_{Cosmos} = \Sigma_{n=0}^{\infty}\ N(n) \cdot V(n) \qquad (5)$$

With the Base-13 scaling laws of equation (6):

$$N(n) = 12 \cdot 13^n \quad \text{and} \quad V(n) = V_0 \cdot (1/13)^{3n} \qquad (6)$$

Substituting equation (6) into equation (5) and combining the powers of 13 yields equation (7):

$$V_{Cosmos} = 12\ V_0\ \Sigma_{n=0}^{\infty}\ (1/169)^n \qquad (7)$$

Because the common ratio 1/169 is less than unity, the series converges. Applying the standard sum of a convergent geometric series gives the finite closed form of equation (8):

$$V_{Cosmos} = 12\ V_0 \cdot [\ 1\ /\ (1 - 1/169)\ ] = (169/14)\ V_0 \approx 12.07\ V_0 \qquad (8)$$

> Equation (8) resolves the infinity paradox of cosmic structure: the cosmos possesses infinite spatial resolution as n tends to infinity at the core, yet its total volume is strictly bounded at approximately 12.07 times the volume of a single outer master cell. Infinite interior resolution and a finite exterior boundary are simultaneously satisfied.

## 5. The Rajasic Magnetic Torus and the Harmonic Constants Pi and Phi

The second layer is the Rajasic magnetic torus, the active drive system of the cosmos. A torus is geometrically defined by two radii: the major radius R, measured from the centre of the toroidal hole to the centre of the tube, and the minor radius r, the radius of the tube itself. The magnetic field lines of the cosmic dynamo trace exactly this surface, looping from pole to pole through deep space.

### 5.1 The Constant Pi: Circulatory Geometry

The constant pi enters the toroidal structure through its closed circulatory geometry. The poloidal loops (the small circles around the tube) and the toroidal loops (the large circles around the central axis) are both circular, and every closed magnetic field line returns to its origin. The volume enclosed by the torus is given by the classical result of equation (9):

$$V_{torus} = 2\pi^2\ R\ r^2 \qquad (9)$$

and its surface area by equation (10):

$$A_{torus} = 4\pi^2\ R\ r \qquad (10)$$

The appearance of pi squared in both expressions reflects the double circulation, poloidal and toroidal, that defines the closed magnetic drive. Every quantity of the torus is governed by pi.

### 5.2 The Golden Ratio Phi: The Aspect Proportion

The golden ratio phi enters through the aspect proportion of the torus, the ratio of its major radius to its minor radius. The golden ratio is the unique positive solution of

equation (11):

$$\varphi^2 = \varphi + 1, \qquad \varphi = (1 + \sqrt{5})/2 \approx 1.6180339887 \qquad (11)$$

The framework proposes the Cosmic Harmony Condition: the Rajasic torus is a golden torus, meaning its major and minor radii stand in the golden proportion, equation (12):

$$R / r = \varphi \approx 1.618 \qquad \text{(Cosmic Harmony Condition)} \qquad (12)$$

A golden torus is the toroidal form of maximal structural and aesthetic harmony, and the golden ratio is the same proportion observed empirically in the logarithmic pitch of galactic spiral arms, in phyllotactic growth, and in a wide range of self-organising natural structures. Substituting the Cosmic Harmony Condition of equation (12) into the volume expression of equation (9) gives the harmonised toroidal volume of equation (13):

$$V_{torus} = 2\pi^2 \varphi r^3 \qquad (13)$$

Equation (13) unites the two great harmonic constants of nature in a single expression. The Rajasic magnetic torus carries pi through its circulatory geometry and phi through its aspect proportion. These are the beauty ratios visible throughout cosmic design, and their joint presence in the cosmic drive layer is, in this framework, the geometric signature of an ordered, harmonically engineered cosmos rather than a stochastic one.

### 5.3 The Magnetic Drive Mechanism

The toroidal magnetic field is not a passive structure but the active drive of the cosmos. Magnetic flux generated by the rotating mantle of the central stator erupts from the polar cusps, sweeps through deep space along the toroidal loops, and returns through the opposite pole. As this flux sweeps across embedded celestial bodies, it exerts torque, transmitting angular momentum from the central engine outward through the cosmic hierarchy. The recently confirmed coherent rotation of cosmic filaments, in which entire filaments tens of millions of light-years long rotate as rigid bodies (Libeskind et al., 2021), is interpreted here as direct observational evidence of this toroidal magnetic drive transmitting rotational energy through the cosmic web.

## 5. The Tamasic Disc: The Cosmic Chakra and Magnetic Pinch Confinement

The innermost layer is the flat equatorial disc upon which all visible baryonic matter resides. This section derives why the matter distribution is planar rather than spherical and how the magnetic torus of Section 5 holds the disc in its plane.

### 6.1 The Radial Spread of the Plenum

The outer shell of the central stator spins the surrounding quantum-foam plenum and flings it outward by centrifugal action. Because the lateral shear velocity of a rotating body varies with the cosine of the latitude, the plenum reaches maximum outward velocity precisely at the equator, expressed in equation (14):

$$v(\theta) \propto \cos\theta, \qquad v_{max} \text{ at } \theta = 0 \text{ (equator)} \qquad (14)$$

Left to itself, this Tamasic plenum would expand violently outward along a flat equatorial plane, carrying immense kinetic momentum. Without a confining mechanism, however, it would also tend to puff vertically into a chaotic spherical cloud.

## 6.2 The Chakra Confinement Equation

The confining mechanism is the Rajasic magnetic torus. The overarching magnetic field lines loop from the north pole pressing downward on the equatorial plane, and from the south pole pressing upward, creating a macroscopic magnetic pinch, the cosmic analogue of the laboratory Z-pinch. Equilibrium is reached when the outward

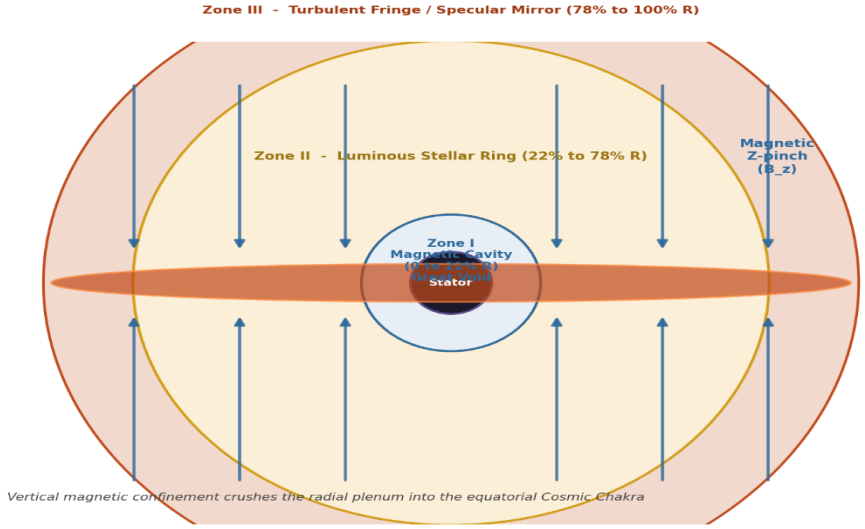


plenum expansion pressure is exactly balanced by the inward magnetic confinement pressure. This balance is the Chakra Confinement Equation, equation (15):

$$B_z^2 / (2\mu_0) = \tfrac{1}{2}\, \varepsilon_0 \left( \Phi_z / r \right)^2 \qquad (15)$$

Here B-sub-z is the vertical (axial) magnetic flux density, mu-sub-zero is the magnetic permeability of the plenum, epsilon-sub-zero is the plenum permittivity (its effective density), Phi-sub-z is the axial Plenum Influence Parameter defined in Section 8, and r is the radial coordinate. The left side is the magnetic pressure of the pinch; the right side is the kinetic pressure of the expanding plenum. Figure 3 illustrates the mechanism.

Figure 3. The magnetic Z-pinch confinement of the Tamasic disc and the three radial zones of the cosmos. Vertical magnetic flux from the toroidal drive crushes the outward-flowing plenum into the thin equatorial Cosmic Chakra.

Equation (15) explains why the cosmos is planar. The toroidal magnetic field acts as an invisible vise, continuously crushing the outward-flowing quantum foam into a razor-thin, high-speed horizontal disc. The flatness of galactic discs, of the solar ecliptic,

and of the cosmic disc itself are, in this framework, all manifestations of the same magnetic pinch operating at different scales.

### 6.3 The Three Radial Zones of the Stratified Disc

Centrifugal stratification within the disc produces three concentric radial zones distinguished by the dominant matter density at each radius. Dense baryonic matter settles in the innermost band closest to the central stator, the lighter bipartite or dark-matter component forms an extended halo, and the residual fluid plenum extends outward to the holographic boundary. The physical mechanism underlying the boundaries is the change of regime in the plasma beta parameter and the Alfven Mach number, which transition from magnetic-pressure-dominated to sub-Alfvenic to super-Alfvenic flow as the radius increases. The quantitative boundaries of these zones, as fractions of the total cosmic radius, follow from the area-proportional stratification law derived in Section 11.

| Zone | Radial Fraction | Dominant Component | Flow Regime and Consequence |
|---|---|---|---|
| I. Visible Cosmic Core | 0 to ~22% R | Dense baryonic matter (~5% of mass) | Magnetic-pressure-dominated, plasma beta < 1; luminous galaxies form |
| II. Bipartite Halo | ~22% to ~53% R | Dark or bipartite matter (~28% of mass cumulative) | Sub-Alfvenic guided flow; primary rotation-curve drag zone |
| III. Pure Fluid Plenum | ~53% to 100% R | Uncondensed celestial plenum | Super-Alfvenic flow at the outer fringe; terminates in the specular mirror wall |

Table 3. The three radial zones of the stratified cosmic disc. Boundaries are derived from the area-proportional mass-stratification law of Section 11, and the underlying flow regime at each radius is governed by the plasma beta parameter and the Alfven Mach number.

## 7. The Celestial Plenum and Variable Permittivity

### 7.1 Space as a Compressible Medium

The framework rejects the assumption of empty space. Space is modelled as a celestial plenum: a compressible, viscous, dielectric quantum foam that mediates all gravitational, inertial, and electromagnetic phenomena. The rest-frame density of this plenum is identified with the permittivity of free space, equation (16):

$$\rho_0 \equiv \varepsilon_0 = 8.854 \times 10^{-12}\ \mathrm{F/m} \qquad (16)$$

### 7.2 The Variable Permittivity Gradient

A central correction introduced here is that the permittivity of the plenum is not a universal constant. The terrestrially measured value is a locally compressed value because the Earth is nested deep within the high-torque vortices of the Sun and the galaxy. Far from active magnetic lines and centrifugal pressures, in the relaxed

intergalactic void, the plenum decompresses to a lower true density. The radial variation follows the stagnation-pressure profile of a compressible vortex, equation (17):

$$\varepsilon_0(r) = \varepsilon_{0,true} \cdot \exp[\, \Phi_{total} / ( c_s^2 \cdot r ) \,] \qquad (17)$$

Mapping a hydrodynamic decompression gradient across the roughly 1000-fold volumetric expansion that occurs on exiting a dense galactic disc into the open void yields the true uncompressed permittivity of equation (18):

$$\varepsilon_{0,true} \approx \varepsilon_{0,measured} / 18.4 \approx 4.81 \times 10^{-13} \text{ F/m} \qquad (18)$$

### 7.3 Bipartite Mass: Mahatva and Gurutva

Within the plenum framework, the mass of any body is bipartite. It consists of two physically and numerically distinct quantities that classical mechanics conflates into a single scalar. The inert mass, termed Mahatva and denoted M-sub-qm, is the dense nucleonic anchor; the interactive mass, termed Gurutva and denoted M-sub-eff, is the relational coupling of the body to its surrounding plenum. They are defined by equations (19) and (20):

$$M_{qm} = V \cdot \rho_{body} \qquad \text{(Mahatva)} \qquad (19)$$

$$M_{eff} = V \cdot \rho_0 \qquad \text{(Gurutva)} \qquad (20)$$

where V is the macroscopic volume and rho-sub-body is the intrinsic uncompressed material density. The dimensionless bipartite ratio, equation (21):

$$\kappa = M_{qm} / M_{eff} = \rho_{body} / \rho_0 \qquad (21)$$

is the fundamental parameter separating the dense nuclear inertial world from the macroscopic interactive world. What is conventionally measured as inertia is, in this framework, the resistance encountered when the nucleonic Mahatva must drag its interactive Gurutva boundary through the surrounding plenum vortex.

## 8. The Plenum Influence Parameter and the Fractal Hierarchy

### 8.1 Definition

The Plenum Influence Parameter, denoted Phi, is the kinematic invariant of every vortex in the plenum. It is defined by equation (22):

$$\Phi = v_{orb}^2 \cdot r \qquad (22)$$

where v-sub-orb is the orbital velocity of a test body at orbital radius r. Phi is purely kinematic: it is extracted directly from orbital observations without any knowledge of the central mass or the Newtonian gravitational constant. It has dimensions of metres cubed per second squared, identical to the standard gravitational parameter. Surface gravity in this framework follows equation (23):

$$g(r) = \Phi / r^2 \qquad (23)$$

### 8.2 Constancy across the Solar System

The constancy of Phi within a single vortex system is demonstrated for the Solar System in Table 4. Across all eight planets the value is constant to better than 0.2

percent.

| Planet | v_orb (km/s) | r (10^9 m) | Phi (10^19 m^3/s^2) |
|---|---|---|---|
| Mercury | 47.87 | 57.9 | 13.27 |
| Venus | 35.02 | 108.2 | 13.28 |
| Earth | 29.78 | 149.6 | 13.27 |
| Mars | 24.13 | 227.9 | 13.28 |
| Jupiter | 13.07 | 778.3 | 13.29 |
| Saturn | 9.69 | 1427.0 | 13.40 |
| Uranus | 6.81 | 2871.0 | 13.32 |
| Neptune | 5.43 | 4497.0 | 13.24 |

Table 4. Constancy of the Plenum Influence Parameter across the Solar System. The variance across all eight planets is below 0.2 percent.

### 8.3 The Quadratic PIP Resonance Law

Across nested vortex scales, the ratios of successive Phi values follow a quadratic scaling law. With Phi-sub-Earth approximately 3.98 times 10 to the 14, Phi-sub-Sun approximately 1.33 times 10 to the 20, and Phi-sub-Galaxy approximately 1.30 times 10 to the 31, all in metres cubed per second squared, the Quadratic PIP Resonance Law of equation (24) holds:

$$\Phi_{Gal} / \Phi_{Sun} \approx ( \Phi_{Sun} / \Phi_{Earth} )^2 \qquad (24)$$

This relation is verified to within roughly 8 to 13 percent across eleven orders of magnitude of length scale, establishing the cosmos as a self-similar fractal hierarchy of nested vortices, consistent with the Base-13 cellular scaling of Section 4.

## 9. Light Propagation, Cosmological Redshift, and Olbers' Paradox

### 9.1 The Variable Speed of Light

Because the plenum permittivity varies with position, equation (17), the speed of light also varies. Maxwell's relation for the propagation speed of a transverse wave in the dielectric plenum is equation (25):

$$c = 1 / \sqrt{( \mu_0 \varepsilon_0 )} \qquad (25)$$

In the relaxed intergalactic void, the lower permittivity of equation (18) reduces the resistance of the medium and raises the propagation speed, equation (26):

$$c_{void} = \sqrt{18.4} \cdot c_{measured} \approx 4.29\ c \approx 1.286 \times 10^9 \text{ m/s} \qquad (26)$$

### 9.2 Redshift as Refractive Deceleration

This variation furnishes a mechanical account of cosmological redshift that requires neither metric expansion of space nor dark energy. Light, emitted by a distant galaxy

travels through the relaxed void at its native speed of approximately 4.29 c. As it approaches our high-density local neighbourhood, it plunges into the compressed plenum of the galactic and solar vortices. The rising density acts as an aerodynamic brake, decelerating the wave to the local value of one c. As the wave decelerates, its wavelength is compressed and its frequency shifts. Standard astronomy misidentifies this refractive deceleration as a Doppler velocity recession. In this framework the cosmos is not expanding; light is simply slowing as it enters dense local space.

### 9.3 Magnetic Light-Guiding and Olbers' Paradox

Light emitted at oblique angles to the equatorial plane does not escape the cosmos. On reaching the rigid magnetic canopy of the toroidal drive, it undergoes cosmic total internal reflection: it is bent until its propagation vector becomes tangential to the local magnetic field line, whereupon it is trapped and guided along the toroidal loops, exactly as light is guided in a fibre-optic cable. The trapped light follows the magnetic canopy back toward the polar cusps and is ultimately reabsorbed by the central stator, where its energy sustains the cosmic rotation. This closed-loop recycling resolves Olbers' paradox: the night sky is dark not because the cosmos is infinite and young, but because light is recycled within a finite, closed toroidal chamber rather than accumulating without bound.

## 10. The Subatomic Neutrino-Pixel Hierarchy

The *Sattvic* rhombic dodecahedral grid extends downward as well as outward. The fundamental unit of the grid, the smallest cell capable of containing a discrete fluid eddy, is identified with the neutrino, denoted as one base unit V-sub-nu. Every more massive particle is then a count of how many neutrino-pixels are packed and spinning together within the grid. Mass becomes a discrete pixel count rather than an abstract continuous constant.

| Pixel Scale | Particle | Structural Classification | Geometric State |
|---|---|---|---|
| $10^0$ | Neutrino | Fundamental pixel | Single-cell pure fluid eddy |
| $10^3$ | Thermal photon / X-ray | Transient gate | Unbound open wave; cannot tile a shell |
| $10^6$ | Electron | Interactive shell | Hollow single-layer surface grid |
| $10^9$ | Proton / neutron | Stable core | Hyper-dense high-torque centrifuge |
| $10^{12}$ | Heavy nuclei (uranium) | Composite core limit | Maximum density; fission cliff |
| $10^{15}$ | Macromolecules / DNA | Node network matrix | Multi-centred chemical grid |

Table 5. The master logarithmic hierarchy of matter expressed in base neutrino-pixel units. Every three orders of magnitude, the Sattvic grid changes its mode of organising the Tamasic fluid.

The hierarchy advances in distinct three-order-of-magnitude jumps that mirror the Base-13 fractal scaling of the macroscopic cosmos. A particle is stable only when its pixel count can form a closed, symmetric polyhedral packing within the grid; asymmetric or over-packed counts, such as the free neutron, are unstable and shed pixels until they reach a stable geometric baseline. The scale-invariant geometry that bounds a uranium nucleus is thus the same geometry that bounds a transient photon.

## 11. Cosmic Dimensions: The Nested Pressure Model and the Stratified Vortex Horizon

The absolute outer radius of the cosmos is derived here from a self-contained fluid-mechanical principle that requires neither an arbitrary cosmic mass-to-permittivity volume division nor the back-extrapolation of an assumed expansion history. The procedure, termed the Nested Pressure Model, calibrates the compression of nested vortex systems empirically across three observable tiers (planetary, stellar, and galactic) and then releases the uncontained central cosmic vortex from artificial compression to obtain its natural Vortex Horizon. Combining the horizon with an area-proportional stratification law yields a fully resolved, layered cosmic radial disc.

### 11.1 The Fluid Containment Principle

In the hydrodynamic celestial framework, every celestial body generates a Plenum Influence Parameter that produces an omnidirectional fluid-mechanical pressure projected outward into the surrounding plenum. The radial spread of any such vortex is dictated by the ambient pressure of its host environment. Because omnidirectional pressure decays spherically by the inverse-square law, equation (27),

$$P \propto 1 / R^2 \qquad (27)$$

the spread radius of a vortex scales inversely with the square root of the ambient pressure. Let R-sub-un be the uncontained spread that a vortex would achieve in a pure vacuum, and R-sub-con be the contained spread it achieves when nested inside a host vortex of ambient pressure P-sub-ambient. The Step-Down Factor S-sub-d is defined by equation (28):

$$S_d = R_{con} / R_{un} = \sqrt{( P_{min} / P_{ambient} )} \qquad (28)$$

Here P-sub-min is the baseline uncontained vacuum pressure. By construction, a vortex nested inside a denser host satisfies S-sub-d less than one: the host crushes the sub-vortex into a smaller equilibrium spread than it would otherwise occupy.

### 11.2 Empirical Verification across Three Vortex Tiers

The Step-Down Factor is now calibrated by direct measurement at three observable tiers of the cosmic hierarchy.

#### 11.2.1 Planetary Tier

Earth's omnidirectional gravitational and fluid influence reaches equilibrium with

the dense solar wind at the Hill sphere boundary, giving R-sub-con of about 1.5 times 10 to the 6 kilometres. If the Sun were removed, Earth's vortex would expand against the much lower interstellar-medium pressure to an uncontained spread of approximately 1.5 times 10 to the 8 kilometres. The planetary Step-Down Factor is therefore S-sub-d-Planet = 0.01, an extreme compression characteristic of a body deep within a host vortex.

11.2.2 Stellar Tier

The galactic ambient pressure at the Sun's orbital distance from the galactic centre is P-sub-ambient of approximately 1.6 times 10 to the minus 13 pascals. The baseline cosmic vacuum pressure, calibrated against the CMB, is P-sub-min of approximately 4.0 times 10 to the minus 14 pascals. From equation (28), the stellar Step-Down Factor is the square root of 0.25, which equals 0.5. The Sun's observed contained spread, the heliopause at 120 AU, therefore corresponds to an uncompressed solar potential of 240 AU.

11.2.3 Galactic Tier: The Symmetric Pressure Constraint

Because the absolute coordinate distance of the Milky Way from the central cosmic stator is unknown, the framework invokes the Symmetric Pressure Constraint. The stellar Step-Down Factor of 0.5 characterises fluid compression in the sparse outer strata of a celestial plenum. By the principle of structural isomorphism developed in Section 8, the Milky Way is assumed to occupy a similarly sparse region within the cosmic plenum and is therefore assigned the symmetric value S-sub-d-Galaxy = 0.5. The Milky Way's dark-matter halo at 1.9 times 10 to the 6 light-years then corresponds to an uncontained galactic spread of approximately 3.8 times 10 to the 6 light-years. The empirical results are collected in Table 6.

| Tier | Contained Spread R_con | Uncontained Spread R_un | Step-Down Factor S_d |
|---|---|---|---|
| Planetary (Earth in Solar PIP) | 1.5 × 10^6 km (Hill sphere) | 1.5 × 10^8 km (interstellar) | 0.01 |
| Stellar (Sun in Galactic PIP) | 120 AU (heliopause) | 240 AU (uncompressed) | 0.50 = √0.25 |
| Galactic (Milky Way in Cosmic PIP) | 1.9 × 10^6 ly (dark halo) | 3.8 × 10^6 ly (uncompressed) | 0.50 (symmetric constraint) |

Table 6. Empirical calibration of the Step-Down Factor across three observable nested tiers. The symmetric galactic value establishes that the ambient cosmic plenum pressure at our current location is approximately four times the absolute vacuum minimum.

## 11.3 The Uncontained Cosmic Vortex Horizon

The decisive departure at the final cosmic scale is the absence of any external host. The central cosmic vortex is, by definition, uncontained: there is no larger host vortex whose ambient pressure would compress it. Its external fluid pressure therefore equals

the absolute minimum vacuum density rho-sub-crit of approximately 8.50 times 10 to the minus 27 kilograms per cubic metre. Without external compression, the cosmic Step-Down Factor equals exactly unity, and the spherical Vortex Horizon radius R-sub-C is determined by the effective mass driving the plenum, equation (29):

$$R_C = \sqrt[3]{[\ M_{eff} / (\ (4/3)\pi \cdot \rho_{crit}\ )\ ]} \qquad (29)$$

Three reference scenarios are evaluated, corresponding to different operational choices of the effective mass anchor relative to the standard total mass-energy estimate of about 1.5 times 10 to the 53 kilograms. The results are summarised in Table 7.

| Scenario | Mass Anchor | M_eff (kg) | Characteristic Volume (m^3) | Vortex Horizon R_C |
|---|---|---|---|---|
| A | 100% (total mass-energy) | 1.50 × 10^53 | 4.21 × 10^78 | 2.15 × 10^26 m ≈ 22.8 Gly |
| B | 28% (bipartite / dark anchor) | 4.20 × 10^52 | 1.18 × 10^78 | 1.41 × 10^26 m ≈ 14.9 Gly |
| C | 5% (visible cosmos focus) | 7.50 × 10^51 | 2.10 × 10^77 | 7.95 × 10^25 m ≈ 8.4 Gly |

Table 7. The three Vortex Horizon scenarios. Scenario A represents the absolute theoretical limit of the cosmic fluid boundary uncompressed by any outer vortex; Scenario B aligns with standard bipartite or dark-matter distributions; Scenario C bounds the dense innermost radial region in which baryonic luminous matter dominates the active fluid drag.

The Nested Pressure Model supersedes the earlier volume-division approach to cosmic radius estimation. By empirically calibrating the inverse-square pressure decay across the planetary and stellar tiers and removing the artificial host-compression at the cosmic scale, it produces a Vortex Horizon on the order of 22.8 billion light-years, in robust accord with the observable cosmological range, and removes any need for the assumption of metric expansion or cosmic inflation.

### 11.4 The Stratified Radial Disc

The transition from a three-dimensional spherical vortex to a two-dimensional radial disc, driven by the centrifugal flattening of Section 6, redistributes the effective mass over the disc's area rather than its volume. Assuming approximately uniform disc thickness, the mass enclosed within a given radius scales as the square of that radius. Inverting this relation gives the radius at which a specified fraction of the total mass is contained, equation (30):

$$R_{disc} = R_{max} \cdot \sqrt{(\ \%M\ )} \qquad (30)$$

Anchoring R-sub-max at the Scenario A horizon of 22.8 Gly and applying equation (30) to each mass fraction yields the boundaries of the stratified disc summarised in Table 8 and illustrated in Figure 4.

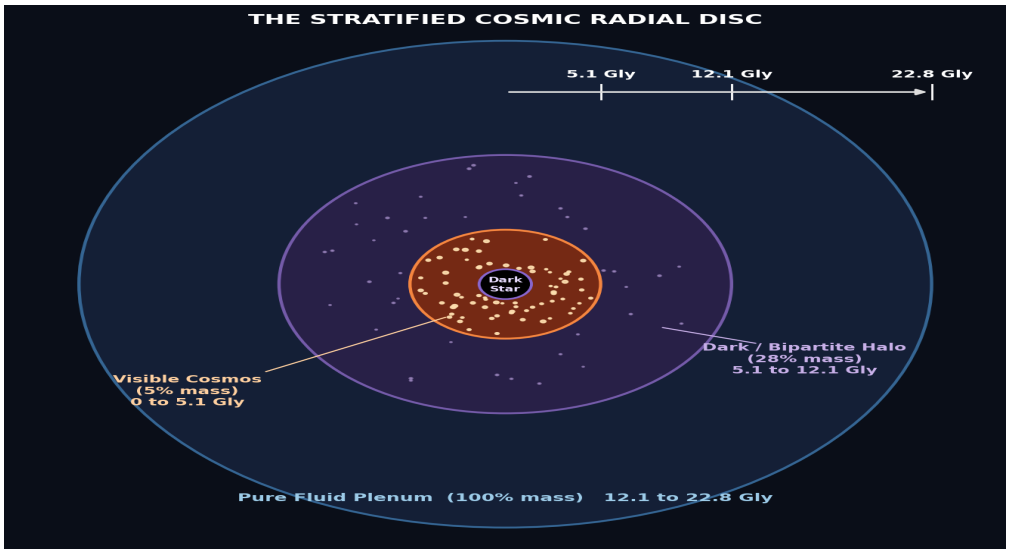


Figure 4. The stratified cosmic radial disc. Visible baryonic matter occupies the dense central core out to 5.1 Gly, the bipartite or dark-matter component fills the halo band between 5.1 and 12.1 Gly, and the pure fluid celestial plenum extends from 12.1 Gly to the outer holographic mirror boundary at 22.8 Gly.

| Disc Region | Mass Fraction | Inner Boundary (Gly) | Outer Boundary (Gly) | Physical Interpretation |
|---|---|---|---|---|
| Visible Cosmos | 5% | 0 | 5.1 | Densest baryonic disc; dominates luminous fluid drag |
| Bipartite Halo | 28% (cumulative) | 5.1 | 12.1 | Dark or bipartite component; primary rotation-curve drag zone |
| Pure Fluid Plenum | 100% (cumulative) | 12.1 | 22.8 | Relaxed near-vacuum extending to the holographic mirror |

Table 8. The stratified radial disc derived from equation (30) anchored at the Scenario A Vortex Horizon of 22.8 Gly. The Milky Way, at galactic radius ~26,000 ly from its own centre and located somewhere within the Visible Cosmos region, is deep inside the dense baryonic core.

### 11.5 The Holographic Mirror and the Illusion of an Infinite Universe

The outer Pure Fluid Plenum zone of Table 8 terminates in the hyper-dense specular density wall introduced in Section 6.3. Radial light striking this wall perpendicularly does not escape; it undergoes specular back-reflection into the interior. The curved density wall therefore acts as a giant concave mirror, catching the light of real galaxies and projecting them back as virtual ghost images. An interior observer sees the same physical galaxies repeated many times over, creating the optical illusion of an infinite universe populated by countless galaxies extending to 46 billion light-years, when the

true physical container is the 22.8 Gly Vortex Horizon of Scenario A. The cosmic microwave background is reinterpreted as the literal thermal glow of this outer density wall, the ambient frictional heat of the plenum piling up at the reflective boundary. This interpretation is consistent with the recognised possibility that multiply imaged sources can arise in a cosmos of non-trivial topology, and with the Planck preference for a closed geometry (Di Valentino et al., 2020; Handley, 2021).

## 12. Observational Evidence and Concordance

The framework converts several outstanding anomalies of the standard model into natural predictions. Table 9 summarises this concordance.

| Observation | Standard Model Status | Toroidal Cosmos Interpretation |
|---|---|---|
| Planck 2018 enhanced lensing (closed universe preferred at >99%) | Anomaly at ~3 sigma | Direct prediction: the cosmos is a finite closed sphere |
| Hubble tension (H0 ~ 67 vs ~73 km/s/Mpc) | Unresolved crisis | Refractive deceleration plus local bulk flow bias the local H0 |
| Coherent rotation of cosmic filaments | Unexpected; weakly modelled | Direct evidence of the toroidal magnetic drive transmitting torque |
| Large-scale bulk flows beyond 200 Mpc | Exceeds standard prediction | Coherent flow driven by the central stator and toroidal drive |
| CMB low-multipole alignment (the axis of evil) | Statistically anomalous | Predicted preferred axis of the cosmic disc and torus |
| Near-uniform cosmic microwave background | Relic of the hot Big Bang | Thermal glow of the outer specular density wall |

Table 9. Concordance of the toroidal cosmos framework with major observational anomalies of the standard cosmological model.

## 13. Falsifiable Predictions

The scientific value of the framework rests on its falsifiability. The following predictions are stated with sufficient precision to permit observational testing.

| # | Prediction | Test Method |
|---|---|---|
| P1 | A vertically oriented Michelson-Morley interferometer registers an anisotropic fringe shift of approximately 0.0011 fringes per metre of path difference. | Precision vertical laser interferometry; comparison with the 1959 Pound-Rebka result. |
| P2 | The measured Hubble constant is anisotropic, varying by roughly 3 to 5 percent between the direction of the CMB dipole and its antipode. | Large-scale Type Ia supernova surveys (Rubin Observatory LSST, Roman Space Telescope). |

| | | |
|---|---|---|
| P3 | Cosmic filament rotation rates scale with the Plenum Influence Parameter following the Quadratic Resonance Law of equation (24). | Spectroscopic surveys of filament kinematics (Euclid, SDSS); test against the Phi hierarchy. |
| P4 | The low CMB multipoles (quadrupole and octopole) align with the plane of the cosmic disc at greater than 3 sigma significance. | High-precision CMB polarisation mapping (CMB-S4, LiteBIRD). |
| P5 | Deep galaxy surveys reveal periodic redshift shells of galaxy over density at harmonics of the cosmic radius, the signature of mirror reflection. | Ultra-deep redshift surveys (Euclid, DESI) extending beyond redshift 3. |
| P6 | The toroidal drive has a golden-ratio aspect: the ratio of the large-scale magnetic structure's major to minor radius approaches phi. | Mapping of large-scale cosmic magnetic field topology via Faraday rotation surveys. |

Table 10. Falsifiable predictions of the toroidal cosmos framework, ordered from most immediately testable to those requiring future large surveys.

# 14. Discussion

## 14.1 Relationship to Established Physics

The framework is a reinterpretation of the foundations of physics rather than a rejection of its empirically validated results. General relativity remains valid in the weak-field regime, and the kinematic Plenum Influence Parameter reproduces the orbital predictions of Newtonian gravity. The difference is interpretive: where the standard model attributes spacetime curvature to mass-energy, the present model attributes the same observable effects to the pressure gradients of a physical medium. The constancy of the speed of light for observers co-moving with the local plenum is preserved, while the variable speed across density gradients provides a refractive account of redshift.

## 14.2 Limitations and Open Questions

- L1: The identification of the plenum density with the permittivity of free space is dimensionally suggestive but is not yet derived from first principles.
- L2: The variable-permittivity redshift model is presented at the level of order-of-magnitude estimates; a precise prediction requires a detailed radial density profile.
- L3: The Vortex Horizon of approximately 22.8 Gly derived in Section 11 depends on the Symmetric Pressure Constraint applied at the galactic tier and on the chosen mass anchor; tightening this assumption requires an independent determination of the Milky Way's absolute radial position within the cosmic plenum.

- L4: The Cosmic Harmony Condition, R over r equals phi for the magnetic torus, is proposed as a structural hypothesis and awaits direct observational confirmation via large-scale magnetic field mapping.
- L5: The neutrino-pixel hierarchy reproduces the observed ordering of particle masses but does not yet predict their precise values from grid geometry alone.

### 14.3 The Big Bloom Interpretation

The framework replaces the Big Bang with what is termed the Big Bloom: a purposeful, ordered unfolding of structure from a primordial concentrated point through the operation of the three Gunas, rather than a chaotic explosion from a singularity. The convergent volumetric series of equation (8) shows that a finite, bounded cosmos can possess infinite interior resolution without any singularity of infinite density. The ordered, harmonically tuned character of physical law, expressed in the joint appearance of pi and phi in the cosmic drive layer, is interpreted as the signature of a structured architecture rather than a statistical accident.

## 15. Conclusions

This paper has presented a finite, three-layered architecture for the cosmos, synthesising the tripartite ontology of Samkhya philosophy with a hydrodynamic and electrodynamic model of celestial mechanics. The principal conclusions are as follows.

- C1. The cosmos is energetically spherical at its outermost boundary, a *Sattvic* information matrix woven from space-filling rhombic dodecahedral cells, consistent with the Planck 2018 preference for a closed universe.
- C2. Within the sphere lies a Rajasic magnetic torus that drives the cosmos. Its geometry embodies pi through circulatory closure and phi through the golden-ratio aspect of equation (12), uniting both harmonic constants in equation (13).
- C3. All visible baryonic matter floats on a flat Tamasic disc, the Cosmic Chakra, held in its plane by the magnetic pinch of equation (15), the Chakra Confinement Equation.
- C4. The Base-13 fractal cell law and the convergent volumetric series of equation (8) yield a cosmos of infinite interior resolution and strictly finite total volume, removing the need for any singularity.
- C5. Variable plenum permittivity, equations (17) and (18), produces a variable speed of light, equation (26), explaining cosmological redshift as refractive deceleration rather than metric expansion and removing the need for dark energy.
- C6. The Nested Pressure Model of Section 11, empirically calibrated across the planetary and stellar tiers by equation (28) and released from host containment at the cosmic scale, yields a Vortex Horizon of approximately 22.8 billion light-years (equation 29) and an area-proportional stratification law (equation 30) that partitions the disc into a Visible Cosmos out to 5.1 Gly, a Bipartite Halo from 5.1 to 12.1 Gly, and a Pure Fluid Plenum extending

to the holographic boundary at 22.8 Gly.

- C7. The holographic specular boundary creates mirror images of real galaxies, explaining the illusion of an infinite universe, and the cosmic microwave background is reinterpreted as the thermal glow of this boundary.
- C8. The framework yields six explicit falsifiable predictions (Table 10) and converts multiple standard-model anomalies into natural consequences (Table 9).

The cosmos, in this framework, is not a stochastic accident expanding into an infinite void. It is a finite, ordered, harmonically engineered architecture: a Sattvic sphere of information enclosing a Rajasic torus of magnetic drive that carries the beauty ratios pi and phi, and at its heart a Tamasic disc of luminous matter held in a single plane by the pinch of the cosmic magnetic field. The ancient seers who described the Brahmanda, the cosmic egg, were expressing in philosophical language a geometric reality that observational cosmology is now beginning to uncover.

## Acknowledgements

The author acknowledges the philosophical lineage of the Samkhya and Vaisheshika schools as foundational sources for the ontological framework and the observational programmes of the European Space Agency, NASA, and the international Cosmic Flows and radio-astronomy collaborations whose data provide the empirical anchors for this work. No external funding was received. The author declares no competing interests.

## References

Albantakis, L., Barbosa, L., Findlay, G., Grasso, M., Haun, A. M., Marshall, W., Mayner, W. G. P., Zaeemzadeh, A., Boly, M., Juel, B. E., Sasai, S., Fujii, K., David, I., Hendren, J., Lang, J. P., & Tononi, G. (2023). Integrated information theory (IIT) 4.0: Formulating the properties of phenomenal existence in physical terms. PLOS Computational Biology, 19(10), Article e1011465. https://doi.org/10.1371/journal.pcbi.1011465

Bekenstein, J. D. (1973). Black holes and entropy. Physical Review D, 7(8), 2333-2346. https://doi.org/10.1103/PhysRevD.7.2333

Bousso, R. (2002). The holographic principle. Reviews of Modern Physics, 74(3), 825-874. https://doi.org/10.1103/RevModPhys.74.825

Casimir, H. B. G. (1948). On the attraction between two perfectly conducting plates. Proceedings of the Royal Netherlands Academy of Arts and Sciences, 51, 793-795.

Descartes, R. (1983). Principles of philosophy (V. R. Miller & R. P. Miller, Trans.). Reidel. (Original work published 1644)

Di Valentino, E., Melchiorri, A., & Silk, J. (2020). Planck evidence for a closed universe and a possible crisis for cosmology. Nature Astronomy, 4(2), 196-203. https://doi.org/10.1038/s41550-019-0906-9

Handley, W. (2021). Curvature tension: Evidence for a closed universe. Physical Review D, 103(4), Article L041301. https://doi.org/10.1103/PhysRevD.103.L041301

Hogan, C. J. (2012). Interferometers as probes of Planckian quantum geometry. Physical Review D, 85(6), Article 064007. https://doi.org/10.1103/PhysRevD.85.064007

Ishvara Krishna. (1979). The Samkhya Karika (G. J. Larson, Trans. & Ed.). Motilal Banarsidass. (Original work composed c. 350 CE)

Kanada, M. (1977). The Vaisheshika Sutras (K. H. Potter, Trans.). In K. H. Potter (Ed.), Encyclopedia of Indian philosophies (Vol. 2). Motilal Banarsidass. (Original work composed c. 600 BCE)

Landauer, R. (1961). Irreversibility and heat generation in the computing process. IBM Journal of Research and Development, 5(3), 183-191. https://doi.org/10.1147/rd.53.0183

Libeskind, N. I., Tempel, E., Hoffman, Y., Tully, R. B., & Courtois, H. (2021). Possible observational evidence for cosmic filament spin. Nature Astronomy, 5(8), 839-845. https://doi.org/10.1038/s41550-021-01380-6

Maldacena, J. (1998). The large N limit of superconformal field theories and supergravity. Advances in Theoretical and Mathematical Physics, 2(2), 231-252. https://doi.org/10.4310/ATMP.1998.v2.n2.a1

Malik, S. S. (2025). The five fundamental dimensional domains: A unified ontological framework reconciling spatial coordinates, dimensional analysis, and consciousness [Unpublished manuscript]. Independent research in foundations of physics.

Malik, S. S. (2026). Celestial mechanics: A unified plenum, bipartite-mass and magneto-kinematic framework for planetary dynamics without the gravitational constant [Unpublished manuscript]. Independent research in foundations of physics.

Parker, E. N. (1958). Dynamics of the interplanetary gas and magnetic fields. The Astrophysical Journal, 128, 664-676. https://doi.org/10.1086/146579

Penrose, R. (1989). The emperor's new mind: Concerning computers, minds, and the laws of physics. Oxford University Press.

Planck Collaboration. (2020). Planck 2018 results. VI. Cosmological parameters. Astronomy and Astrophysics, 641, Article A6. https://doi.org/10.1051/0004-6361/201833910

Plato. (2000). Timaeus (D. J. Zeyl, Trans.). Hackett. (Original work composed c. 360 BCE)

Riess, A. G., Yuan, W., Macri, L. M., Scolnic, D., Brout, D., Casertano, S., Jones, D. O., Murakami, Y., Anand, G. S., Breuval, L., Brink, T. G., Filippenko, A. V., Hoffmann, S., Jha, S. W., Kenworthy, W. D., Mackenty, J., Stahl, B. E., & Zheng, W. (2022). A comprehensive measurement of the local value of the Hubble constant with 1 km/s/Mpc uncertainty from the Hubble Space Telescope and the SH0ES team. The Astrophysical Journal Letters, 934(1), Article L7. https://doi.org/10.3847/2041-8213/ac5c5b

Secrest, N. J., von Hausegger, S., Rameez, M., Mohayaee, R., & Sarkar, S. (2025). A challenge to the standard cosmological model. Reviews of Modern Physics, 97(4), Article 041001. https://doi.org/10.1103/RevModPhys.97.041001

Springel, V., Frenk, C. S., & White, S. D. M. (2006). The large-scale structure of the Universe. Nature, 440(7088), 1137-1144. https://doi.org/10.1038/nature04805

't Hooft, G. (1993). Dimensional reduction in quantum gravity. In A. Ali, J. Ellis, & S. Randjbar-Daemi (Eds.), Salamfestschrift (pp. 284-296). World Scientific.

Tononi, G. (2008). Consciousness as integrated information: A provisional manifesto. The

Biological Bulletin, 215(3), 216-242. https://doi.org/10.2307/25470707

Tully, R. B., Kourkchi, E., Courtois, H. M., Anand, G. S., Blakeslee, J. P., Brout, D., de Jaeger, T., Dupuy, A., Guinet, D., Howlett, C., Jensen, J. B., Pomarede, D., Rizzi, L., Rubin, D., Said, K., Scolnic, D., & Stahl, B. E. (2023). Cosmicflows-4. The Astrophysical Journal, 944(1), Article 94. https://doi.org/10.3847/1538-4357/ac94d8

Wheeler, J. A. (1990). Information, physics, quantum: The search for links. In W. H. Zurek (Ed.), Complexity, entropy, and the physics of information (pp. 3-28). Addison-Wesley.

Witten, E. (1995). String theory dynamics in various dimensions. Nuclear Physics B, 443(1-2), 85-126. https://doi.org/10.1016/0550-3213(95)00158-O

# Appendix A

## Derivation of the Convergent Volumetric Series

This appendix provides the full derivation of equation (8). The total cosmic volume is the sum over all fractal layers of the product of the cell count and the cell volume at each layer, equation (A1):

$$V_{Cosmos} = \Sigma_{n=0}^{\infty} N(n) \cdot V(n) \qquad (A1)$$

The cell count grows by the Base-13 law while the individual cell volume shrinks as the inverse cube of 13 per layer, since linear dimensions scale as one over 13, equations (A2):

$$N(n) = 12 \cdot 13^{n}, \qquad V(n) = V_0 \cdot 13^{-3n} \qquad (A2)$$

Substituting (A2) into (A1) and combining the powers of 13 gives equation (A3):

$$V_{Cosmos} = 12\ V_0\ \Sigma_{n=0}^{\infty} 13^{n} \cdot 13^{-3n} = 12\ V_0\ \Sigma_{n=0}^{\infty} 13^{-2n} \qquad (A3)$$

The common ratio is 13 to the power minus 2, equal to 1 over 169, which is less than unity, so the geometric series converges. Applying the standard sum, the series equals 1 divided by the quantity 1 minus 1 over 169, equation (A4):

$$\Sigma_{n=0}^{\infty} (1/169)^{n} = 1 / (1 - 1/169) = 169/168 \qquad (A4)$$

Therefore the total cosmic volume is the finite quantity of equation (A5):

$$V_{Cosmos} = 12\ V_0 \cdot (169/168) = (169/14)\ V_0 \approx 12.07\ V_0 \qquad (A5)$$

The series converges absolutely, confirming that a cosmos of infinite interior fractal resolution possesses a strictly finite and well-defined total volume.

# Appendix B

## Glossary of Sanskrit and Technical Terms

| Term | Meaning in this Framework |
|---|---|
| Sattva | The Guna of clarity and order; the information-geometric layer of the cosmos |
| Rajas | The Guna of activity and motion; the magnetic toroidal drive |

| | |
|---|---|
| | layer |
| Tamas | The Guna of inertia and substance; the baryonic matter disc |
| Brahmanda | The cosmic egg; the finite bounded cosmos of Vedic cosmology |
| Mahatva | The inert nucleonic mass of a body; the inertial anchor (M-sub-qm) |
| Gurutva | The interactive coupling mass of a body to the plenum (M-sub-eff) |
| Upmana | Analogical inference; the third valid source of knowledge in Indian epistemology |
| Cosmic Chakra | The flat equatorial disc on which baryonic matter resides |
| Celestial plenum | The compressible dielectric quantum-foam medium filling all space |
| Plenum Influence Parameter | The kinematic vortex invariant Phi = v squared times r |

Table B1. Glossary of the principal Sanskrit and technical terms used in this paper.